Inorganic Chemistry

Article

pubs.acs.org/IC

H_4octapa: Highly Stable Complexation of Lanthanide(III) Ions and Copper(II)

Ferenc Krisztián Kálmán,[†] Andrea Végh,[†] Martín Regueiro-Figueroa,[‡] Éva Tóth,[§] Carlos Platas-Iglesias,*[,‡] and Gyula Tircsó*[,†]

[†]Department of Inorganic and Analytical Chemistry, University of Debrecen, Egyetem tér 1, H-4010 Debrecen, Hungary

[‡]Departamento de Química Fundamental, Universidade da Coruña, Campus da Zapateira, Rúa da Fraga 10, 15008 A Coruña, Spain

[§]Centre de Biophysique Moléculaire, CNRS, rue Charles Sadron, 45071 Cedex 2 Orléans, France

Supporting Information

ABSTRACT: The acyclic ligand octapa^{4-} (H_4octapa = 6,6′-((ethane-1,2-diylbis((carboxymethyl)azanediyl))bis-(methylene))dipicolinic acid) forms stable complexes with the Ln^{3+} ions in aqueous solution. The stability constants determined for the complexes with La^{3+}, Gd^{3+}, and Lu^{3+} using relaxometric methods are log K_{LaL} = 20.13(7), log K_{GdL} = 20.23(4), and log K_{LuL} = 20.49(5) (I = 0.15 M NaCl). High stability constants were also determined for the complexes formed with divalent metal ions such as Zn^{2+} and Cu^{2+} (log K_{ZnL} = 18.91(3) and log K_{CuL} = 22.08(2)). UV−visible and NMR spectroscopic studies and density functional theory (DFT) calculations point to hexadentate binding of the ligand to Zn^{2+} and Cu^{2+}, the donor atoms of the acetate groups of the ligand remaining uncoordinated. The complexes formed with the Ln^{3+} ions are nine-coordinated thanks to the octadentate binding of the ligand and the presence of a coordinated water molecule. The stability constants of the complexes formed with the Ln^{3+} ions do not change significantly across the lanthanide series. A DFT investigation shows that this is the result of a subtle balance between the increased binding energies across the 4f period, which contribute to an increasing complex stability, and the parallel increase of the absolute values of the hydration free energies of the Ln^{3+} ions. In the case of the $[Ln(octapa)(H_2O)]^-$ complexes the interaction between the amine nitrogen atoms of the ligand and the Ln^{3+} ions is weakened along the lanthanide series, and therefore the increased electrostatic interaction does not overcome the increasing hydration energies. A detailed kinetic study of the dissociation of the $[Gd(octapa)(H_2O)]^-$ complex in the presence of Cu^{2+} shows that the metal-assisted pathway is the main responsible for complex dissociation at pH 7.4 and physiological $[Cu^{2+}]$ concentration (1 μM).

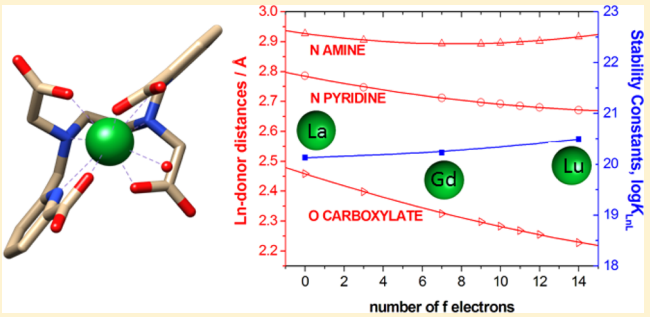

INTRODUCTION

The introduction of Gd^{3+} complexes as contrast agents in magnetic resonance imaging (MRI) has quickly revolutionized the field of clinical diagnostics, as it has allowed establishing new routine protocols for noninvasive diagnosis.[1] The wide scope and the impact in health care of MRI has stimulated thriving investigation activities on Gd^{3+} complexes and other inorganic paramagnetic species, particularly Mn^{2+}, Fe^{2+}, and Fe^{3+}-based compounds.[2,3] The viability of paramagnetic complexes as efficient contrast agents is subjected to several conditions:[4] (i) the presence of water molecules directly coordinated to the metal center with a proper exchange rate with bulk water, which is related with the contrast enhancement efficiency of the contrast agent; (ii) high thermodynamic stability and kinetic inertness of the complex, which relate to the safe in vivo use of the agent.[1] The problem of Gd^{3+} toxicity associated with the administration of contrast agents is receiving much attention in the last years, due to the recently described disease nephrogenic systemic fibrosis (NSF), associated with the dissociation in vivo of Gd^{3+}-based contrast agents in patients with severe renal failure.[5] In the case of Gd^{3+} complexes with nonmacrocyclic ligands endogenous metal ions such as Zn^{2+} and Cu^{2+} play a catalytic role in the dissociation of the contrast agent under physiological conditions.[6]

About a decade ago, one of us reported the octadentate ligand 6,6′-((ethane-1,2-diylbis((carboxymethyl)azanediyl))bis-(methylene))dipicolinic acid (H_4octapa, Chart 1) and its complexation properties toward the lanthanide ions.[7] It was shown that the picolinate moieties of this ligand can sensitize both the Eu^{3+} and Tb^{3+} luminescence, while the Gd^{3+} complex shows relaxivities comparable to or slightly higher than those of commercially available contrast agents. Later, Mazzanti et al. reported the X-ray structure of the Gd^{3+} complex, as well as the thermodynamic stability constants of the Ca^{2+} and Gd^{3+} complexes with this ligand. The stability of the Gd^{3+} complex

Received: December 11, 2014

DOI: 10.1021/ic502966m
Inorg. Chem. XXXX, XXX, XXX−XXX

Chart 1. Chemical Structures of the Ligands Discussed in This Work

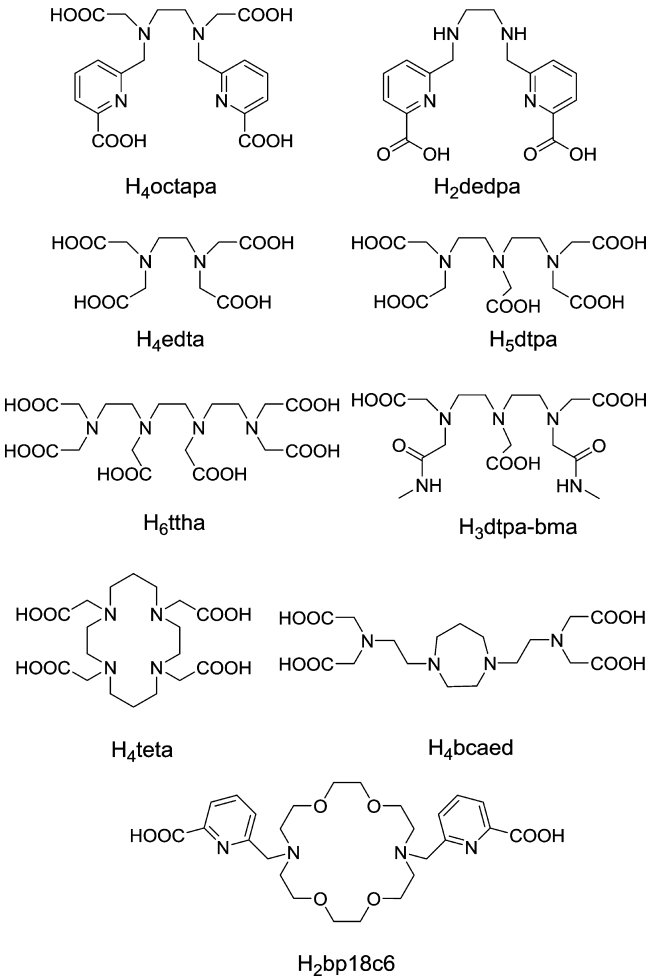

was found to be too low for its application as a contrast agent in MRI (log K_{Gd} = 15.1).[8] More recently Orvig et al. investigated the $[In(octapa)]^-$ complex, which was shown to possess a very high thermodynamic stability (log K_{In} = 26.8) and very promising properties for the preparation of ^{111}In-based radiopharmaceuticals.[9,10] Furthermore, the related ligand H_2dedpa (Chart 1), first reported by Platas-Iglesias et al.,[11] was also shown to have ideal properties for ^{68}Ga PET imaging elaboration[12] and high complexation affinity toward ^{64}Cu.[13] In vitro competition experiments with human blood serum showed that the complex of H_4octapa with ^{177}Lu is >85% stable at 24 h.[14] Furthermore, a recent determination of the stability constant of the Lu^{3+} complex of $octapa^{4-}$ pointed to a rather high thermodynamic stability of this complex (log K_{Lu} = 20.1).[14a]

Considering the favorable coordination properties of H_4octapa and 1,2-[{6-(carboxylato-)pyridin-2-yl}-methylamino]ethane (H_2dedpa) toward different divalent and trivalent metal ions, the low stability reported for the Gd^{3+} analogue is rather surprising. Thus, in this work the equilibrium properties of the H_4octapa ligand and its metal complexes formed with several Ln^{3+} ions were reexamined. The complexes were found to be substantially more stable than expected on the basis of the data reported by Mazzanti et al. To understand the stability trend observed along the lanthanide series, several $[Ln(octapa)(H_2O)]^-$ complexes were also investigated by using density functional theory (DFT) calculations. The stability constants of the complexes formed by this ligand with different biogenic metal ions (Mg^{2+}, Ca^{2+}, Zn^{2+}, and Cu^{2+}) were also determined. The kinetic inertness of the $[Gd(octapa)]^-$ complex was also addressed by studying metal exchange reactions between the complex and Cu^{2+}.

RESULTS AND DISCUSSION

Synthesis of the Ligand. Ligand H_4octapa was synthesized by N-alkylation of the precursor **1** (Scheme 1) with *tert*-butyl-2-bromoacetate at room temperature in acetonitrile solution, followed by the deprotection of the methyl and *tert*-butyl esters with 6 M HCl. The ligand was isolated with an overall yield of 59% over the two steps, which represents an important improvement with respect to the previously reported procedure in which the alkylation reaction was conducted in refluxing acetonitrile (21%).[7] The use of milder alkylation conditions requires longer reaction times (several days), but improves considerably the yield of the reaction most likely minimizing the formation of lactams and quaternary ammonium salts as a result of polyalkylation. A recent synthesis of H_4octapa reported by Orvig starting from *tert*-butyl ester derivative of **1** proceeded with an overall yield of 71%.[15] However, the strategy followed by Orvig requires the preparation of *tert*-butyl 6-(bromomethyl)picolinate, which was isolated in 40% yield after radical bromination of the corresponding methyl derivative with *N*-bromosuccinimide.

Ligand Protonation Constants and Stability Constants of the Metal Complexes. The protonation constants of $octapa^{4-}$ were measured by using the standard pH-potentiometric technique in 0.15 M NaCl, which is considered to mimic the conditions present in biological fluids better than other electrolyte solutions. The ligand protonation constants are defined as in eq 1.

Scheme 1. [a]

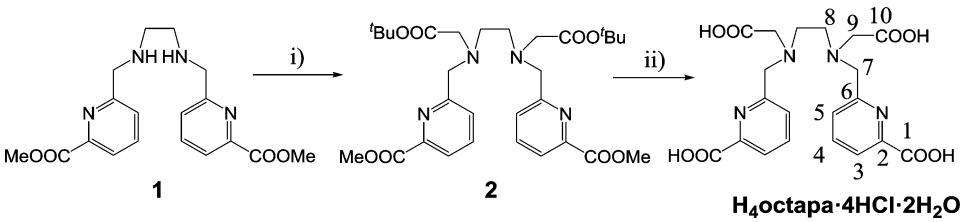

[a]Reagents and conditions: (i) *tert*-butyl-2-bromoacetate (2.1 equiv), K_2CO_3, acetonitrile, room temperature, 4 d and 45 °C, 3 d; (ii) 6 M HCl, reflux, 24 h.

DOI: 10.1021/ic502966m
Inorg. Chem. XXXX, XXX, XXX−XXX

$$K_i^H = \frac{[H_iL]}{[H_{i-1}L][H^+]} \quad (1)$$

The protonation constants obtained in 0.15 M NaCl are in good agreement with the data published by Mazzanti et al.[8] in 0.1 M KCl and more recently by Orvig and co-workers,[9] even though the salts used to set the ionic strength in the samples were different (Table 1). This experimental finding can be explained by the absence of any complex formation between the ligand and both Na^+ and K^+ ions (or their similar affinity toward the octapa^{4-} ligand).

Table 1. Protonation Constants of octapa^{4-} and the Related Ligands (25 °C, 0.15 M NaCl)

	octapa^{4-} [a]	octapa^{4-}	edta^{4-} [a]	dtpa^{5-} [b]
log K_1^H	8.52(1)	8.5,[c] 8.59[d]	9.18(3)	9.93
log K_2^H	5.40(1)	5.2,[c] 5.59[d]	6.00(4)	8.37
log K_3^H	3.65(1)	3.5,[c] 3.77[d]	2.58(5)	4.18
log K_4^H	2.97(1)	2.9,[c] 2.77[d]	2.29(4)	2.71
log K_5^H	1.66(1)	2.79[d]		2.00
$\sum$log K_i^H	22.20	20.1,[c] 23.51[d]	20.05	27.19

[a]This work, 0.15 M NaCl; standard deviations are given in parentheses. [b]0.15 M NaCl from ref 16. [c]0.1 M KCl from ref 8. [d]Reference 9.

The protonation constants of the octapa^{4-} ligand are considerably lower than those of the related octadentate dtpa^{5-} ligand (dtpa = diethylenetriaminepentaacetic acid), which is the result of the electron-withdrawing effect of the picolinate moieties also evidenced in the literature for numerous macrocyclic picolinates studied previously.[17] In fact, the sum of the total basicities of edda^{2-} ($\sum$log K_i^H = 20.31, edda = ethylenediamine-*N*,*N*′-diacetate)[18] and two picolinic acids ($\sum$log K_i^H = 5.26(2) × 2)[19] is orders of magnitude higher than that determined for the octapa^{4-} ligand, which shows that the replacement of two acetate pendants of edta^{4-} (edta = ethylenediaminetetraacetic acid) by picolinates results in a noticeable decrease of the basicity of the nitrogen donor atoms of the ligand.

The stability constants of the metal chelates and the protonation constants of the complexes are expressed by eqs 2 and 3, respectively.

$$K_{ML} = \frac{[ML]}{[M][L]} \quad (2)$$

$$K_{MH_iL} = \frac{[MH_iL]}{[MH_{i-1}L][H^+]} \text{ with } i = 1, 2 \quad (3)$$

Furthermore, the potentiometric data obtained in the presence of metal ion excess also indicated the formation of dinuclear species (except for Mg^{2+}), which were characterized as expressed in eq 4.

$$K_{M_2L} = \frac{[M_2L]}{[ML][M]} \quad (4)$$

The stability constants of the complexes formed with Mg^{2+} and Ca^{2+} ions could be determined by applying the direct pH-potentiometric method. Simultaneous fitting of the titration curves obtained at different metal-to-ligand ratios indicated the formation of mononuclear (ML) complex species and their mono- and diprotonated (MHL and MH_2L) forms. However, the fitting of the titration data of the Ca^{2+} system could be improved considering the formation of the dinuclear (Ca_2L) complex, which indicates the formation of the given species in the samples with metal-to-ligand ratio greater than 1. The stability of the $[Mg(octapa)]^{2-}$ complex was found to be 1−2 orders of magnitude lower than those of the $[Mg(edta)]^{2-}$ or $[Mg(dtpa)]^{3-}$ complexes, while the Ca^{2+} ion forms complexes of similar stability with these ligands (Table 2).

Table 2. Protonation and Stability Constants of the Metal Complexes Formed with octapa^{4-}, edta^{4-}, and dtpa^{5-} Ligands (25 °C, 0.15 M NaCl)

	octapa^{4-}	edta^{4-}	dtpa^{5-}
log K_{LaL}	19.92(6)[a]	14.48[b]	19.48[c]
	20.13(7)[d]		
log K_{GdL}	20.23(4)[e]	16.28[b]	22.03[f]
	20.39(9)[g]		
	15.1[h]		
log K_{LuL}	20.49(5)[d]	18.19[b]	22.44[c]
	20.08[i]		
log K_{MgL}	6.12(1)	7.75[j]	8.56[j]
log K_{MgHL}	5.24(1)		6.97[j]
log K_{MgH_2L}	4.54(2)		4.68[j]
log K_{CaL}	9.55(1)	9.36[j]	9.82[j]
	9.4[h]		
log K_{CaHL}	3.92(1)		5.98[j]
log K_{CaH_2L}	2.56(3)		4.43[j]
log K_{Ca_2L}	1.55(8)		1.77[j]
log K_{ZnL}	18.91(3)[d]	14.61[j]	17.58[f]
log K_{ZnHL}	3.91(3)		5.37[f]
log K_{ZnH_2L}	3.54(2)		2.38[f]
log K_{Zn_2L}	2.3(1)		4.33[f]
log K_{CuL}	22.08(2)[k]	18.8[l]	23.40[f]
log K_{CuHL}	3.95(6)		4.63[f]
log K_{CuH_2L}	3.21(6)		2.61[f]
log K_{Cu_2L}	3.2(1)		6.56[f]

[a]Values obtained using spectrophotometry. [b]25 °C, 0.5 M $NaClO_4$ from ref 21. [c]25 °C, 0.1 M KCl from ref 24. [d]Obtained using a relaxometric competitive titration with Gd^{3+}. [e]Obtained using relaxometric titrations. [f]25 °C, 0.15 M NaCl from ref 16. [g]Competitive titration by using the ttha^{6-} ligand (the stability constants used for the determination are included in the Supporting Information). [h]From ref 8. [i]From ref 14. [j]37 °C, 0.15 M NaCl form ref 22. [k]Competitive titration with the use of cyclen (the stability constants used for the determination are included in the Supporting Information). [l]20 °C, 0.1 M $NaClO_4$ from ref 23.

Owing to the very high stability constants (found to form quantitatively already below pH < 1.8) of the complexes formed with Zn^{2+}, Cu^{2+}, La^{3+}, Gd^{3+}, and Lu^{3+}, spectrophotometric and relaxometric methods (competition methods) were applied to determine the stability constants. The results of equilibrium studies are summarized in Table 2. The stability constant of the $[Zn(octapa)]^{2-}$ complex was determined by relaxometry with the use of Gd^{3+} ion as a competing metal ion (vide infra). Interestingly, the value of the stability constant for $[Zn(octapa)]^{2-}$ is the highest among the complexes investigated and compared in this study (octapa^{4-}, edta^{4-} and dtpa^{5-}), which shows that the structure of the ligand offers the best coordination environment for the Zn^{2+} ion. On the other hand, the stability of the $[Cu(octapa)]^{2-}$ complex was found to

DOI: 10.1021/ic502966m
Inorg. Chem. XXXX, XXX, XXX−XXX

be exceptionally high forcing us to use a competition method involving another ligand for stability constant determination. The equilibrium in the system Cu^{2+}:cyclen:H^+ (cyclen = 1,4,7,10-tetraazacyclododecane) was revisited by us recently (Supporting Information) and the constants obtained agree well with the data published elsewhere.[20] Preliminary experiments indicated that the given ligand may be a good competing partner in this system, and therefore samples containing equimolar amounts of octapa^{4-} and Cu^{2+} and various amounts of cyclen were prepared in the pH range of 10−11 (Supporting Information). The samples were set aside for a couple of days to allow the equilibrium to be attained. Subsequently, the absorption spectra were acquired in the wavelength range of 400−875 nm, and the spectral data and stability constant of the [Cu(octapa)]$^{2-}$ complex were determined by using the molar absorption coefficients of the different light-absorbing species. The fitting of the data returned a stability constant of log K([Cu(octapa)]$^{2-}$) = 22.08, a value being approximately 1 order of magnitude lower than that of [Cu(dtpa)]$^{3-}$ (Table 2). Nevertheless, the low basicity of the octapa^{4-} ligand results in very high conditional stability constants of the Cu^{2+} complex species formed with this ligand. As a result, the diprotonated [Cu(H_2octapa)] complex represents up to 99.3% of the overall Cu^{2+} in a 1 M HCl solution (92.7% in 5 M or 80.8% in 10 M HCl not considering the possible Cl^- competition under these conditions), which makes the given ligand an excellent candidate for Cu^{2+} ion complexation under highly acidic conditions.

The determination of the stability constant of the [Gd(octapa)]$^-$ complex was carried out by using two different approaches. First, the stability constant of the given complex was determined by a direct relaxometric method following the changes in relaxivity as a function of pH (in the pH range of 0−12; pH in the acidic samples equals to $-\log c_{H+}$). The results presented in Figure 1 clearly show that the relaxivity of the

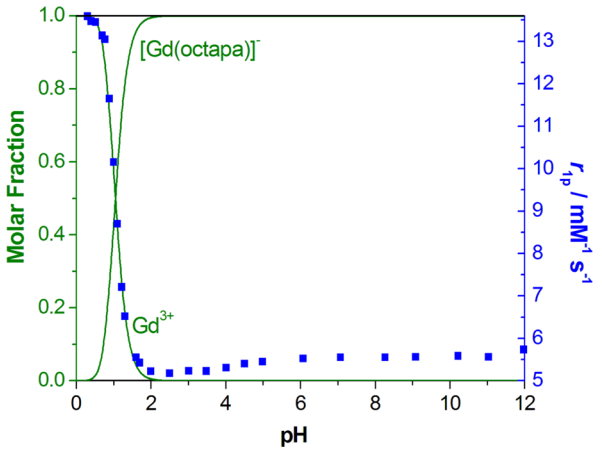

Figure 1. Species distribution curves and relaxivity values (blue ■) as a function of pH (25 °C, 20 MHz) determined for the [Gd(octapa)]$^-$ complex.

[Gd(octapa)]$^-$ complex is fairly constant between pH 1.8 and 12, the small fluctuations observed (<0.5 mM^{-1} s^{-1}) being close to the error of the measurement (~5%). This suggests that no protonation or deprotonation occurs in the quoted pH range, which is confirmed by potentiometric titrations. Below pH 1.8 a significant increase in relaxivity is observed, which is related to the dissociation of the complex and Gd^{3+} release. The relaxivity value of the [Gd(octapa)]$^-$ complex at 20 MHz and 25 °C was found to be 5.5 mM^{-1} s^{-1}, which is in agreement with the presence of one inner-sphere water molecule. This is consistent with the relaxivity value published earlier for this complex,[7] as well as with its X-ray crystal structure.[8] The stability constant determined using this method (Table 2) showed a large discrepancy with the value reported previously by Chatterton et al.[8] Thus, the stability constant of the [Gd(octapa)]$^-$ complex was also determined by using a competitive method employing the ttha^{6-} ligand (ttha = triethylenetetramine-*N*,*N*,*N*′,*N*″,*N*‴,*N*⁗-hexaacetic acid, Chart 1; the data characterizing the equilibrium in the system Gd^{3+}:ttha^{6-}:H^+ are included in the Supporting Information). The competition method returned a stability constant that is in excellent agreement with the one determined by direct relaxometry (log K [Gd(octapa)]$^-$ = 20.39(9) vs 20.23(4) determined by the relaxometric method). Furthermore, these data are also close to the stability constant published recently by C. Orvig and co-workers for the Lu^{3+} complex,[14] which indicates that the stability published by Chatterton et al. was underestimated by ca. 5 log K units.[8]

The large difference in the stability constants can be explained by the very high conditional stability of the complex, which results in the formation of complex species under highly acidic solutions (pH < 1.6), where the measurement of pH is doubtful. It is important to note however that Chatterton et al. performed the pH-potentiometric titrations in the pH range of 2.5−8.5 by using considerably lower concentrations (5.0×10^{-4} M) than those employed in the current study and overlooked the fact that crystals obtained by them from very acidic samples (ca. pH = 1) showed complexation of Gd^{3+} by the ligand.

Relying on the stability constant of the [Gd(octapa)]$^-$ complex, the formation constants of the Zn^{2+}, La^{3+}, and Lu^{3+} complexes could also be determined by using a relaxometric competition method with Gd^{3+} as a challenging metal ion. In the case of the Ln^{3+} ions the titration data could be successfully analyzed by assuming the formation of [Gd(octapa)]$^-$ as the only complex species present in the equilibrium, while for the Zn^{2+} and Cu^{2+} complexes protonated and dinuclear species were detected. To test the reliability of the relaxometric competition method, the stability constants of [La(octapa)]$^-$ were also determined by means of spectrophotometric measurements. These experiments were carried out under acidic conditions by following the changes in the $\pi \rightarrow \pi^*$ absorption band of the picolinate chromophore. Both methods returned results in very good agreement (Table 2). Interestingly, the stability constants of the complexes formed with different ions along the lanthanide series (La^{3+}, Gd^{3+}, and Lu^{3+}) were found to be very similar, so that the stability constants of the lighter versus heavier Ln^{3+} ions do not differ significantly. This is rather unusual in the light of the trends usually observed in the stability constants of lanthanide(III) polyamino−polycarboxylate complexes along the series.[25] It is important to note that the stability constants of the [Ln(octapa)]$^-$ complexes are orders of magnitude higher than those of the corresponding edta^{4-} complexes, which can be explained in terms of higher denticity of octapa^{4-} in comparison with the denticity of the edta^{4-} ligand, which shows that the replacement of two acetate pendants arms by picolinates does contribute to the stability of the complexes. By comparing the stability of the corresponding octapa^{4-} complexes with the data published for the dtpa^{5-} analogues, similar (for the lighter metal ions) or slightly smaller (ca. 2 log

DOI: 10.1021/ic502966m
Inorg. Chem. XXXX, XXX, XXX−XXX

Scheme 2. Assumed Reaction Mechanisms of the Dissociation of Gd^{3+} Complexes (charges are omitted for clarity)

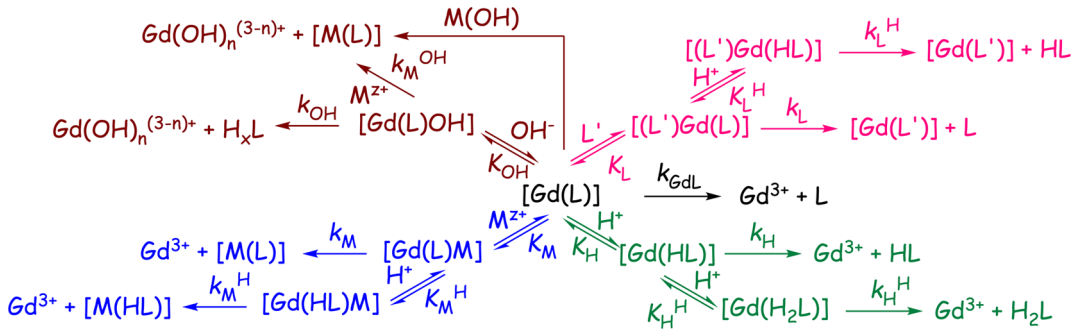

K units) stability constants are observed along the lanthanide series. However, we emphasize that the octapa^{4-} ligand is considerably less basic, so that the conditional stability constants of [Ln(octapa)]$^{-}$ complexes are higher than those of the complexes formed with the dtpa^{5-} ligand. This can also be demonstrated by calculating and comparing the corresponding pGd values (pGd = −log[Gd^{3+}(free)] by using c_L = 10 μM, c_{Gd3+} = 1 μM, and pH = 7.4) for the octapa^{4-}, edta^{4-}, and dtpa^{5-} systems: 20.2 ([Gd(octapa)]$^{-}$), 14.9 ([Gd(edta)]$^{-}$, see Supporting Information), and 19.4 ([Gd(dtpa)]$^{2-}$).[16]

Kinetic Measurements. A high kinetic inertness is an important property of MRI relaxation agents that is usually characterized by the rate of dissociation of the complexes under certain conditions. To obtain information on the kinetic inertness of the [Gd(octapa)]$^{-}$ complex we investigated the transmetalation reactions occurring between the complex and a suitable exchanging metal ion (Cu^{2+} ion). The dissociation reactions (eq 5) were studied in the presence of high excess (10−50 fold) of Cu^{2+} as an exchanging metal ion to ensure the pseudo-first-order conditions.

$$[Gd(octapa)]^{-} + Cu^{2+} \rightleftharpoons [Cu(octapa)]^{2-} + Gd^{3+} \quad (5)$$

In the presence of such high excess of the exchanging metal ion the rate of dissociation can be expressed by eq 6, where k_{obs} is the observed pseudo-first-order rate constant, and $[GdL]_{tot}$ is the total concentration of the [Gd(octapa)]$^{-}$ complex.

$$-\frac{d[GdL]_{tot}}{dt} = k_{obs}[GdL]_{tot} \quad (6)$$

In general the dissociation of metal complexes may occur via the following pathways: spontaneous dissociation, acid catalyzed (and rarely hydroxide-assisted) dissociation, and metal ion initiated decomplexation or transmetalation, which involves the direct attack of the exchanging metal ion on the complex.[26] Furthermore, endogenous ligands (e.g., HCO_3^-, $H_2PO_4^{2-}$, $HCit^{2-}$, etc.) were also found recently to accelerate the dissociation of certain Gd^{3+} complexes.[27] Our preliminary experiments performed with the [Gd(octapa)]$^{-}$ complex indicated that the exchange reactions are much faster than in the [Gd(dtpa)]$^{2-}$complex, and thus in the current study we did not consider the catalytic effect of these endogenous anions and focused on metal exchange reactions only. In transmetalation reactions the exchanging metal attacks directly the complex forming a key dinuclear intermediate [Gd(L)M] in the initial step. This intermediate can dissociate directly releasing the Gd^{3+} ion or may pick up a proton at low pH, so that dissociation occurs following the so-called proton-metal-assisted pathway. Furthermore, the catalytic effect of the $Cu(OH)^{+}$ species formed at low concentration may also be observed when using the Cu^{2+} ion as a ligand scavenger at pH ≥ 4.6. By taking into account the dissociation pathways mentioned above, the overall map of dissociation can be illustrated by the general scheme shown in Scheme 2.

By considering each pathway in Scheme 2 the concentration of the [Gd(octapa)]$^{-}$ complex can be written as the sum of the concentrations of the different reactive species as follows:

$$\begin{aligned}[Gd(L)]_{tot} = {} & [GdL] + [Gd(HL)] + [Gd(H_2L)] \\ & + [Gd(L)M] + [Gd(HL)M] + [Gd(L)L'] \\ & + [Gd(HL)L'] + [GdOH(L)] \\ & + [Gd(L)MOH] \end{aligned} \quad (7)$$

Combination of eqs 6 and 7 gives

$$\begin{aligned}-\frac{d[Gd(L)]_t}{dt} = {} & k_{obs}[Gd(L)]_{tot} = k_{GdL}[Gd(L)] \\ & + k_H[Gd(HL)] + k_H^H[Gd(H_2L)] + k_{OH}[Gd(OH)(L)] \\ & + k_M^{OH}[Gd(L)M(OH)] + k_M[Gd(L)M] \\ & + k_M^H[Gd(HL)M] + k_L[Gd(L)L'] + k_L^H[Gd(HL)L'] \end{aligned} \quad (8)$$

The different rate constants given in eq 8 characterize the rate of the spontaneous (k_{GdL}), proton-assisted (k_H, k_H^H), hydroxide-assisted (k_{OH}), hydroxide-metal-assisted, (k_M^{OH}) metal-assisted (k_M), proton-metal-assisted (k_M^H), ligand (k_L), and proton-ligand-assisted (k_L^H) pathways. Inspection of the pseudo-first-order rate constants obtained as a function of acid and metal ion concentration indicates that the rate constant characterizing the spontaneous dissociation cannot be determined from the kinetic data, as the reaction involving the $Cu(OH)^{+}$ species emerged to be a competing reaction to the spontaneous dissociation in the samples with pH ≥ 4.6. The hydroxide-catalyzed dissociation may also be ruled out because of the extremely high stability of the [Gd(octapa)]$^{-}$ complex, along with the absence of the formation of any ternary hydroxo complexes in the samples of Ln^{3+} ions titrated up to pH = 12.0. Taking into account these considerations, the reaction pathways depicted in Scheme 2 and the expressions for the equilibrium constants K_H, K_H^H, K_M, K_M^H, and $K_{M(OH)}$, the pseudo-first-order rate constants (k_{obs}) can be expressed as follows:

DOI: 10.1021/ic502966m
Inorg. Chem. XXXX, XXX, XXX−XXX

$$k_{obs} = \{k_0 + k_1[H^+] + k_2[H^+]^2 + k_3[M^{n+}] + k_4[M][H^+] + k_6[M(OH)]\}/\{1 + K_H[H^+] + K_H K_H^H[H^+]^2 + K_M[M] + K_M^H[M][H^+] + K_{M(OH)}[M(OH)]\} \quad (9)$$

where $k_0 = k_{GdL}$, $k_1 = k_H K_H$, $k_2 = k_H^H K_H K_H^H$, $k_3 = k_M K_M$, $k_4 = k_M^H K_H$, $k_6 = k_M^{OH} K_{M(OH)}$, $K_H = [Gd(HL)]/[Gd(L)][H^+]$, $K_H^H = [Gd(H_2L)]/[Gd(HL)][H^+]$, $K_M = [Gd(L)M]/[Gd(L)][M]$, and $K_{M(OH)} = [Gd(L)M(OH)]/[Gd(L)][M(OH)]$

Figure 2 shows the best fit of the k_{obs} values to eq 9. In the fitting process k_0, k_4, K_H^H, K_M, K_M^H, and $K_{M(OH)}$ were found to be

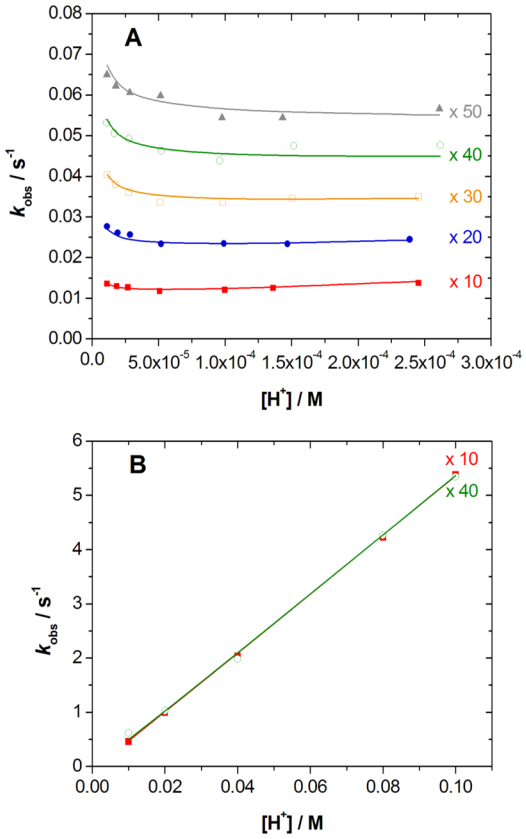

Figure 2. Dependence of the pseudo-first-order rate constants on the concentration of H^+ ions for the metal-exchange reaction between $[Gd(octapa)]^-$ and the Cu^{2+} ion (25 °C, 0.15 M NaCl). The excess of the Cu^{2+} ion was ×10, ×20, ×30, ×40, and ×50-fold (A) and ×10 and × 40-fold (B).

negligible, and therefore these constants were omitted during the calculations. Besides, it was not possible to determine the rate constant characterizing the acid-catalyzed dissociation pathway (k_1), as the pseudo-first-order rate constants obtained in the pH range of 3.6−5.0 were practically independent of the acid concentration (except for the slight increase in the k_{obs} for the samples with higher pH owing to the catalytic effect of the $Cu(OH)^+$ species, see Figure 2a). To obtain data for the acid-catalyzed dissociation, metal-exchange reactions were also explored at much higher acid concentration (in $[H^+]$ range of 0.01−0.1 M). As a result of the high stability of the $[Cu(octapa)]^{2-}$ complex the exchange reactions occur to a 100% extent even in the given acid concentration range. Under these conditions the reactions were found to be independent of the metal ion concentration (Figure 2b), which is not very surprising since complex dissociation in highly acidic medium occurs predominantly via the acid-catalyzed pathway, while at high pH the metal-exchange pathway dominates.

The results of the fitting of k_{obs} to eq 9 are presented in Table 3, where the rate constants for the dissociation of $edta^{4-}$ and $dtpa^{5-}$ complexes are also shown for comparison. The rate constants characterizing the acid- and metal-ion-catalyzed dissociation show that dissociation of the $[Gd(octapa)]^-$ complex is faster (~20 times) than that of $[Gd(dtpa)]^{2-}$. However, the rate constants characterizing the acid-catalyzed dissociation (k_1 and k_2) of $[Gd(edta)]^-$ are considerably higher than those found for $[Gd(octapa)]^-$, which is probably a consequence of the lower basicity of the $octapa^{4-}$ ligand. In contrast to this, the comparison of the values of k_3 for the $[Gd(edta)]^-$ and $[Gd(octapa)]^-$ complexes shows that the replacement of two acetate moieties in $edta^{4-}$ by picolinates units increases the rate of the metal-ion-catalyzed dissociation pathway in the resulting complex. This is very likely the result of the higher denticity of the ligand, which favors the formation of the key dinuclear intermediate. Furthermore, the fitting of the pseudo-first-order rate data returned a high protonation constant (log K_H = 2.6(1)) characterizing the intermediate in the proton-assisted dissociation pathway. However, our attempts to include the monoprotonated complex in the equilibrium model used to fit the pH-potentiometry and relaxometric data were unsuccessful. Thus, it is likely that the protonated complex is present in solution at low concentration but has a significant kinetic activity in the decomplexation process.

Table 3. Rate and Equilibrium Constants Characterizing the Dissociation of the Gd^{3+} Complexes of $octapa^{4-}$, $edta^{4-}$, and $dtpa^{5-}$ (25 °C)[a]

	$octapa^{4-}$	$edta^{4-}$	$dtpa^{5-}$ [b]
k_1 (M^{-1} s^{-1})	11.8 ± 2.4	87[c]	0.58
k_2 (M^{-2} s^{-1})	(2.5 ± 0.7) × 10^4	6 × 10^6 [c]	9.7 × 10^4
k_3^{Cu} (M^{-1} s^{-1})	22.5 ± 0.5	1.3 × 10^{-2} (Tb)[d]	0.93
k_6^{Cu} (M^{-2} s^{-1})	(5.0 ± 0.8) × 10^9		
log K_H	2.6 ± 0.1		1.3
$t_{1/2}$ (h)[e]	0.15	55	202

[a]The errors given correspond to the standard deviations obtained from the least-squares fits of the experimental data. [b]Reference 6. [c]Reference 28. [d]Reference 29. [e]The half-life of the Gd^{3+} complexes were calculated at physiological conditions, pH = 7.4, $c_{Cu^{2+}}$ = 1 μM.

The presence of various dissociation pathways characterized by their corresponding rate constants makes the direct comparison of the kinetic inertness of different Gd^{3+} complexes difficult. Therefore, the half-life ($t_{1/2}$) values of the dissociation reactions calculated at physiological conditions (pH = 7.4 and at $c_{Cu^{2+}}$ = 1 × 10^{-6} M concentration of the exchanging Cu^{2+} ion) are presented in Table 3. The data clearly show that the kinetic inertness of the $[Gd(octapa)]^-$ complex is more than 2 orders of magnitude lower than that of $[Gd(edta)]^-$ or $[Gd(dtpa)]^{2-}$, mainly because of the significant contribution of the metal exchange mechanism to the decomplexation reaction. In biological media the Cu^{2+} ion is found predominantly in complexed forms (complexes formed with bioligands, amino acids, proteins, etc.), and hence the contribution of the pathway involving the $Cu(OH)^+$ species is likely to play a minor role. By neglecting the pathway involving $Cu(OH)^+$ a half-life of 8.4 h can be estimated for $[Gd(octapa)]^-$. Moreover, the half-life of

DOI: 10.1021/ic502966m
Inorg. Chem. XXXX, XXX, XXX−XXX

the dissociation can easily be increased to 17 d by neutralizing the effect of the exchanging metal ion completely with the use of slight ligand excess (few percent). This procedure is not new in clinical practice, as this strategy is used for the administration of the commercially available MRI contrast agent Omniscan ([Gd(dtpa-bma)]), or the radiopharmaceutical Multibone ($[^{153}Sm(edtmp)]^{5-}$), used for the palliative treatment of painful bone metastases of different tumors in vivo.[30]

Density Functional Theory Calculations on the [Ln(octapa)](H$_2$O)]$^-$·2H$_2$O Systems. Aiming to understand the reasons behind the unusual stability trend observed for Ln^{3+} complexes with octapa^{4-} along the lanthanide series, we performed theoretical calculations based on the hybrid meta-GGA functional TPSSh. In a previous work we reported a DFT study of the [Gd(octapa)](H$_2$O)]$^-$·xH$_2$O systems (x = 0−2) and showed that the explicit inclusion of two second-sphere water molecules was crucial for an accurate computation of Gd−O$_{water}$ distances and ^{17}O hyperfine coupling constants of the coordinated water molecule.[31] Thus, in this work we have extended these calculations to the [Ln(octapa)](H$_2$O)]$^-$·2H$_2$O systems, where Ln = La, Nd, Dy, Ho, Er, Tm, and Lu, which were fully optimized by using the previously reported optimal DFT geometry of the Gd^{3+} analogue (Figure 3, see also Figure S4, Supporting Information).

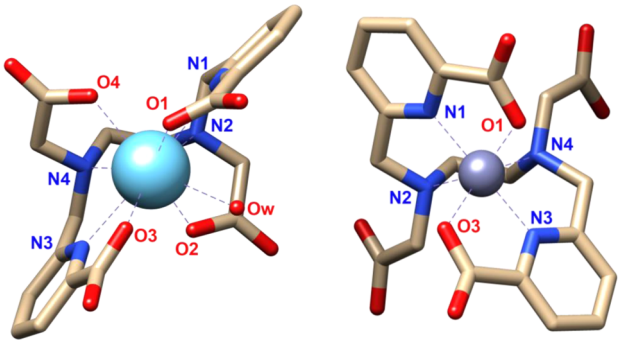

Figure 3. Structures of the [La(octapa)(H$_2$O)]$^-$·2H$_2$O (left) and [Zn(octapa)]$^{2-}$ (right) complexes optimized in aqueous solution using DFT calculations. Hydrogen atoms and noncoordinated water molecules were omitted for simplicity.

The bond distances of the metal coordination environment calculated for the [Ln(octapa)](H$_2$O)]$^-$·2H$_2$O systems provide clear evidence that the interaction between some donor atoms of the ligand and the Ln^{3+} ion is weakened as the ionic radius of the metal ion decreases (Figure 4, see also Table S5, Supporting Information). Indeed, most of the distances between the Ln^{3+} ions and the donor atoms of the ligand decrease along the lanthanide series, as usually observed for Ln^{3+} complexes as a consequence of the lanthanide contraction.[32] However, the distances between the Ln^{3+} and the amine nitrogen atoms N2 and N4 decrease on decreasing the ionic radius from La^{3+} to Gd^{3+}, but then slightly increase from Gd^{3+} to Lu^{3+}. Thus, the interaction between the metal ion and several of the donor atoms of octapa^{4-} is weakened as the ionic radius of the metal ion decreases, which points to a better match between the binding sites offered by the ligand structure and the binding sites required by large Ln^{3+} ions. An increase of Ln−N$_{amine}$ bond distances along the lanthanide series has been observed previously for Ln^{3+} complexes with macrocyclic ligands, and in some instances this resulted in an unprecedented selectivity for the largest ions.[17a,33]

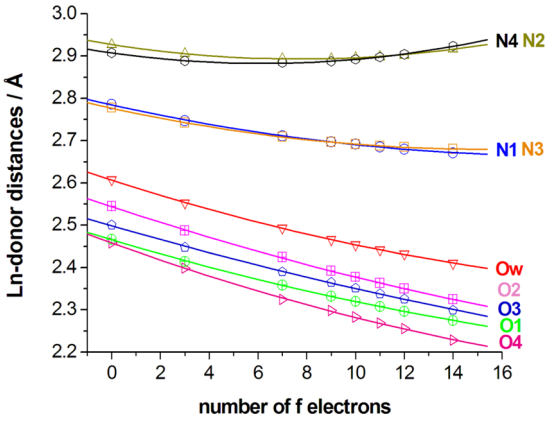

Figure 4. Variation of the calculated bond distances of the metal coordination environments for the [Ln(octapa)(H$_2$O)]$^-$·2H$_2$O systems at the TPSSh/LCRECP/6-31G(d,p) level. The solid lines represent quadratic fits of the data to $y = a + bx + cx^2$ with $R^2 > 0.999$.

The average values of the nine bond distances of the metal coordination environments plotted against the number of f electrons of the Ln^{3+} ion give an excellent quadratic fit of the form $y = a + bx + cx^2$ with $R^2 > 0.999$ (Figure S5 and Table S6, Supporting Information). The quadratic fit provides the following parameters: a = 2.663(1), $b = -1.50(2) \times 10^{-2}$, and $c = 3.68(14) \times 10^{-4}$, which results in normalized parameters of $b^* = b/a = -5.62 \times 10^{-3}$ and $c^* = c/a = 1.38 \times 10^{-4}$. These values fall between those obtained for the complexes with ligands bp18c6^{2-} and becaed^{4-},[25] which are very selective for the lightest and heaviest Ln^{3+} ions, respectively, in line with the intermediate behavior observed for the [Ln(octapa)(H$_2$O)]$^-$ complexes.

Aiming to gain further insight into the reasons behind the stability trend observed for Ln^{3+} complexes of octapa^{4-} across the 4f period, we performed an energy analysis using the following thermodynamic cycle.[25]

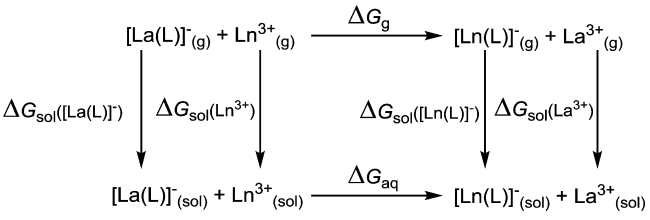

where ΔG_g and ΔG_{aq} represent the Gibbs free energies in the gas phase and water solution for the reaction involving the La^{3+} complex and a given Ln^{3+} ion, and ΔG_{sol} is the hydration free energy of the different species. The ΔG_g values become more negative on proceeding to the right across the lanthanide series, which is a result of the increased positive charge density of the metal ion. However, the ΔG_g(Lu) value obtained for the complexes with octapa^{4-} (−96.81 kcal·mol^{-1}) is less negative than those calculated for complexes whose stability increases along the lanthanide series ($\Delta G_{g(Lu)}$ = −107.8 and −114.7 kcal·mol^{-1} for [Ln(teta)]$^-$ and [Ln(becaed)]$^-$ complexes, respectively),[25] which is explained by the weakening of the Ln−N$_{amine}$ bonds across the series in [Ln(octapa)(H$_2$O)]$^-$ complexes. On the other hand, the ΔG_g(Lu) value obtained for the bp18c6^{2-} complexes, whose stability decreases dramatically across the series, is clearly lower in absolute sense (−88.89 kcal·mol^{-1}). Furthermore, the hydration free energies of the [Ln(octapa)(H$_2$O)]$^-$·2H$_2$O systems do not change significantly along the series, while the hydration free energies of the Ln^{3+} ions

DOI: 10.1021/ic502966m
Inorg. Chem. XXXX, XXX, XXX−XXX

become more negative from −788.1 kcal mol^{-1} for La^{3+} to −888.1 kcal mol^{-1} for Lu^{3+}.[34] As a result, in aqueous solution the ΔG_{aq} values remain fairly constant across the lanthanide series. These results therefore are in perfect agreement with the similar thermodynamic stabilities determined for the La^{3+}, Gd^{3+}, and Lu^{3+} complexes of octapa^{4-}. It is worth noting the ΔG_{aq} values calculated using the structures of [Ln(octapa)-(H_2O)]$^-$·2H_2O optimized in the gas phase and in solution are very similar (Table 4).

Table 4. Thermodynamic Data Obtained with DFT Calculations at the TPSSh/LCRECP/6-31G(d,p) Level (kcal mol^{-1})

Ln	ΔG_g [a]	ΔG_{sol}(LnL) [b]	ΔG_{sol}(LnL) [c]	ΔG_{aq}^{cald} [b]	ΔG_{aq}^{cald} [c]
La	0.00	−85.00	−89.84		
Nd	−25.97	−85.37	−90.28	2.06	2.00
Gd	−54.52	−85.54	−90.20	2.04	2.21
Dy	−68.62	−85.62	−89.69	2.57	3.33
Tm	−86.50	−85.23	−89.27	2.47	3.27
Lu	−96.81	−85.13	−89.22	3.06	3.81

[a]BSSE corrections taken into account with the counterpoise method. [b]ΔG_{sol}(LnL) were calculated in aqueous solution using the structures optimized in vacuo at the TPSSh/LCRECP/6-31G(d,p) level. [c]ΔG_{sol}(LnL) were calculated in aqueous solution using the structures optimized in solution at the TPSSh/LCRECP/6-31G(d,p) level.

Solution Structure of the Zn^{2+} and Cu^{2+} Complexes. Considering the high stability of the Zn^{2+} and Cu^{2+} complexes with octapa^{4-}, we carried out a spectroscopic and theoretical study to gain information on their solution structures. Thus, the ^{1}H and ^{13}C NMR spectra of the Zn^{2+} complex of octapa^{4-} were recorded from a D_2O solution at 298 K (pD = 7.0), and peaks were assigned on the basis of two-dimensional COSY, NOESY, HSQC, and HMBC experiments. The spectra are shown in Figure 5, and the results are summarized in Table 5. The proton spectrum consists of nine signals corresponding to the 18 different proton magnetic environments of the ligand backbone, which points to an effective C_2 symmetry of the complex in solution. This is confirmed by the ^{13}C NMR spectrum, which shows 10 signals for the 20 carbon nuclei of the ligand backbone (Table 5). The methylene protons H7ax/H7eq and H9ax/H9eq (see Scheme 1 for labeling) are diastereotopic and provide AB spin patterns (^2J = 17 and 18 Hz, respectively), while the protons of the ethylenediamine units H8ax/H8eq give an AA′BB′ spectrum, where the signal due to the equatorial protons are deshielded due to the polarization of the C−H bonds by the electric field effect caused by the cation charge. This points to a relatively rigid structure of the [Zn(octapa)]$^{2-}$ complex in aqueous solution.

The coordination of the ligand to the metal ion causes important downfield shifts of the protons of the pyridine units, which points to the coordination of the picolinate groups to the Zn^{2+} ion (Figure 5). The signal due to the carbonyl carbon atoms of the picolinate units C1 experiences a highfield shift of 4.0 ppm upon coordination to the Zn^{2+} ion, while the signal due to the carbonyl group of the acetate arms undergoes a relatively small upfield shift (1.2 ppm). A very important upfield shift (6.9 ppm) is also observed for the carbon nuclei of the pyridyl unit C2. Taken together, these observations suggest that the octapa^{4-} ligand binds to the Zn^{2+} ion through the donor atoms of the picolinate groups and the amine nitrogen atoms, the donor atoms of the acetate arms remaining

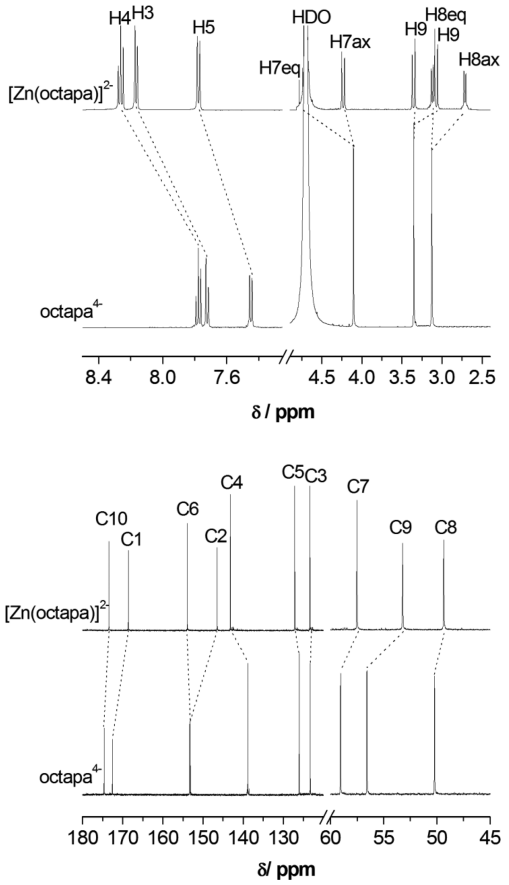

Figure 5. ^{1}H (upper) and ^{13}C (lower) NMR spectra of [Zn(octapa)]$^{2-}$ and octapa^{4-} recorded in D_2O solution at 298 K (pD = 7.0). See Scheme 1 for labeling.

uncoordinated. DFT calculations performed at the TPSSh/TZVP level provide an optimized structure with a C_2 symmetry and a distorted octahedral geometry at the metal center (N_4O_2, Figure 3). The bond distances and angles of the metal coordination environment (Table S5, Supporting Information) are quite similar to those observed in the solid state for [Zn(dedpa)].[11] Theoretical calculation of the ^{13}C shielding tensors using the GIAO method provides chemical shifts in very good agreement with the experimental values, which confirms the octahedral coordination of the ligand to Zn^{2+} in aqueous solution (Table 5).

The optimized geometry of the [Cu(octapa)]$^{2-}$ complex resembles that of the Zn^{2+} analogue, with the metal ion being six-coordinated by the donor atoms of the picolinate moieties. However, two of the bond distances of the metal coordination environment involving donor atoms of the ligand in trans positions (Cu−O1 and Cu−N2) are considerably longer. This is characteristic of octahedral Cu^{2+} complexes that present Jahn−Teller distortion, as observed in the solid state for the [Cu(dedpa)] complex.[13] Further support for the octahedral coordination of the ligand to Cu^{2+} is provided by the absorption spectra of the [Cu(octapa)]$^{2-}$ and [Cu(dedpa)] complexes (Figure 6). Indeed, the two complexes present a broad d−d absorption band with maxima at 728 nm (ε = 98 M^{-1} cm^{-1}) and 715 nm (ε = 66 M^{-1} cm^{-1}), respectively. The similar position and intensity of the d−d absorption band in the two complexes point to similar coordination environments. Furthermore, although the plasticity of Cu^{2+} makes difficult the

DOI: 10.1021/ic502966m
Inorg. Chem. XXXX, XXX, XXX−XXX

Table 5. ^{1}H and ^{13}C NMR Shifts for Ligand Octapa^{4-} and Its Zn^{2+} Complex[a]

^{1}H	octapa^{4-}	[Zn(octapa)]$^{2-}$ [b]	^{13}C	octapa^{4-}	[Zn(octapa)]$^{2-}$ [c]	[Zn(octapa)]$^{2-}$ [d]
H3	7.72	8.16	C1	172.6	168.6	170.8
H4	7.78	8.26	C2	153.3	146.5	151.3
H5	7.45	7.77	C3	123.3	123.4	122.8
H7ax	4.11	4.23	C4	138.8	143.2	142.2
H7eq	4.11	4.70	C5	126.1	127.2	126.8
H8ax	3.13	2.71	C6	153.2	154.0	158.5
H8eq	3.13	3.12	C7	59.1	57.5	60.7
H9	3.35	3.08	C8	50.2	49.4	50.6
H9′	3.35	3.36	C9	56.6	53.2	55.6
			C10	174.6	173.5	176.8

[a]Conditions: T = 298 K, D_2O, 500 MHz. [b]$^{3}J_{3-4} = {}^{3}J_{5-4}$ = 7.8 Hz; $^{2}J_{7ax\text{-}7eq}$ = 17.2 Hz; $^{2}J_{8ax\text{-}8eq}$ = 11.6 Hz; $^{2}J_{9-9'}$ = 17.7 Hz. [c]Experimental values. [d]Theoretical shifts obtained with GIAO calculations in aqueous solution at the TPSSh/TZVP level.

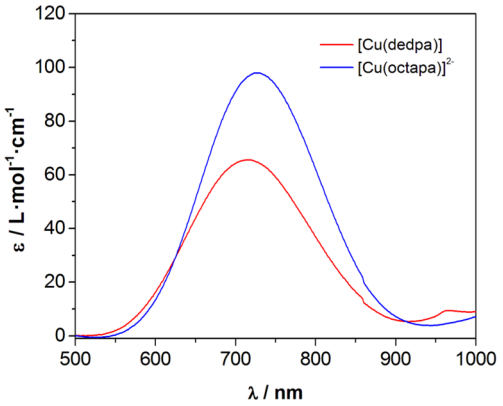

Figure 6. UV−vis spectra of the [Cu(dedpa)] and [Cu(octapa)]$^{2-}$ complexes recorded in aqueous solution at 298 K and pH 7.0.

inference of structural features from electronic data, the position of these absorption bands is consistent with an octahedral coordination.[35]

CONCLUSIONS

The [Ln(octapa)(H_2O)]$^{-}$ complexes present thermodynamic stabilities that are comparable to those of commercially available contrast agents such as [Gd(dtpa)(H_2O)]$^{2-}$. The stability constants of [Ln(octapa)](H_2O)]$^{-}$ complexes remain fairly constant along the series, which reflects the balance of two opposite effects: (i) the increased charge density of the metal ion as its ionic radius decreases, which often results in an increasing stability of the complexes on proceeding to the right across the series and (ii) the weakening of the Ln−N_{amine} bonds across the series. Ligand octapa^{4-} also forms very stable complexes with metal ions such as Zn^{2+} and Cu^{2+} as a result of the hexadentate binding of the ligand through the donor atoms of the picolinate groups and the amine nitrogen atoms. Kinetic studies have shown that the [Gd(octapa)(H_2O)]$^{-}$ complex is considerably more labile than the edta^{4-} and dtpa^{5-} counterparts. As often observed for complexes with nonmacrocyclic chelators,[26] dissociation under physiological conditions occurs mainly through metal-assisted (Cu^{2+}) pathways, both due to a direct attack of the exchanging metal ion with the formation of a dinuclear intermediate and the catalytic role of the $Cu(OH)^{+}$ species. However, these dissociation pathways are expected to play a limited role in biological media due to the very low concentration of uncomplexed Cu^{2+}.

EXPERIMENTAL AND COMPUTATIONAL SECTION

Materials and Methods. 6,6′-((Ethane-1,2-diylbis(azanediyl))bis-(methylene))dipicolinic acid (**1**) and H_2dedpa were prepared according to the published procedures.[7,11] All other chemicals were purchased from commercial sources and used without further purification, unless otherwise stated. Elemental analyses were carried out on a Carlo Erba 1108 elemental analyzer. Electrospray ionization time-of-flight (ESI-TOF) mass spectra were recorded using an LC-Q-q-TOF Applied Biosystems QSTAR Elite spectrometer in the positive mode. UV−vis spectra were recorded on PerkinElmer Lambda 900 or Varian Cary 1E spectrophotometers in 1.0 cm path quartz cells. IR spectra were recorded on a Bruker Vector 22 instrument with an ATR accessory. ^{1}H and ^{13}C NMR spectra were recorded at 25 °C on a Bruker Avance 500 MHz spectrometer. Spectral assignments were based in part on two-dimensional COSY, HSQC, NOESY, and HMBC experiments.

6,6′-((Ethane-1,2-diylbis((carboxymethyl)azanediyl))bis-(methylene))dipicolinic acid (H_4octapa·4HCl·2H_2O). A mixture of **1** (1.00 g, 2.79 mmol) and K_2CO_3 (3.39 g, 24.6 mmol) in acetonitrile (100 mL) was stirred for 30 min, and then *tert*-butyl-2-bromoacetate (1.14 g, 5.86 mmol) was added. The mixture was stirred at room temperature for 4 d under an inert atmosphere (Ar) and later at 45 °C for a period of 3 d. The excess K_2CO_3 was removed by filtration, the filtrate was concentrated to dryness, and the yellow oil was extracted with a 1:3 mixture of H_2O and $CHCl_3$ (200 mL). The organic phase was evaporated to dryness to give **2** as a yellow oil (1.20 g). A solution of compound **2** (1.20 g, 2.05 mmol) in 6 M HCl (50 mL) was heated to reflux for 24 h, and then the solvent was concentrated in a rotary evaporator to ∼5 mL, which resulted in the precipitation of a white solid. It was collected by filtration and dried under vacuum to give H_4octapa·4HCl·2H_2O (1.04 g) as a white solid. Yield: 59%. Anal. Calcd for $C_{20}H_{22}N_4O_8$·4HCl·2H_2O: C 38.23, H 4.81, N 8.92%. Found: C 37.86, H 4.83, N 8.92%. MS (ESI^{+}, MeOH/CH_3CN/H_2O 9:1:1): m/z 447.15; calculated for $[C_{20}H_{23}N_4O_8]^{+}$ 447.15. IR (ATR): ν 1725 cm^{-1} (C═O). ^{1}H NMR (D_2O, pD 7.0, 500 MHz, 25 °C, TMS): δ 7.78 (t, 2H, ^{3}J = 7.8 Hz), 7.72 (dd, 2H, ^{3}J = 7.8 Hz, ^{4}J = 0.9 Hz), 7.45 (dd, 2H, ^{3}J = 7.8 Hz, ^{4}J = 0.9 Hz), 4.11 (s, 4H), 3.35 (s, 4H), 3.13 ppm (s, 4H). ^{13}C NMR (D_2O, pD 7.0, 125.8 MHz, 25 °C, TMS): δ 174.6, 172.6, 153.3, 153.2, 138.8, 126.1, 123.3, 59.1, 56.6, 50.2 ppm.

Equilibrium Measurements. The chemicals used in the studies were of the highest analytical grade. The $LnCl_3$ solutions were prepared by dissolving Ln_2O_3 (Fluka, 99.9%) in 6.0 M HCl and evaporating the excess of acid. The concentration of the metal chloride solutions were determined by complexometric titration with the use of a standardized Na_2H_2EDTA solution and xylenol orange ($LnCl_3$, $ZnCl_2$), murexid ($CuCl_2$), and Patton & Reeder ($CaCl_2$) as indicators.[36]

The pH-potentiometric titrations were carried out with a Methrohm 888 Titrando titration workstation using a Metrohm-6.0233.100 combined electrode. The titrated solutions (10.00 mL) were thermostated at 25 °C. The samples were stirred and kept under inert gas atmosphere (N_2) to avoid the effect of CO_2. For the pH

DOI: 10.1021/ic502966m
Inorg. Chem. XXXX, XXX, XXX−XXX

calibration of the electrode, KH-phthalate (pH = 4.005) and borax (pH = 9.177) buffers were used.

The concentration of the H_4octapa ligand was determined by pH-potentiometric titration. The protonation constants of octapa^{4-}, the stability and protonation constants of the complexes formed with Mg^{2+} and Ca^{2+}, as well as the protonation constants of Cu^{2+} and Zn^{2+} complexes and formation constants of their dinuclear complexes were determined by pH-potentiometric titration. The metal-to-ligand concentration ratios were 1:1 and 2:1 (the concentration of the ligand was generally 3−4 mM). In the pH-potentiometric titrations 50−100 mL:pH data pairs were recorded in the pH range of 1.7−12.0. The calculation of $[H^+]$ from the measured pH values was performed with the use of the method proposed by Irving et al.[37] by titrating a 0.01 M HCl solution (I = 0.15 M NaCl) with a standardized NaOH solution. The differences between the measured and calculated pH values were used to obtain the $[H^+]$ concentrations from the pH data obtained in the titrations. The ion product of water was determined from the same experiment in the pH range of 11.4−12.0. The protonation and stability constants were calculated from the titration data with the PSEQUAD program.[38]

The determination of the stability constants of $[Ln(octapa)]^-$ complexes was carried out using ^{1}H-relaxometric and UV−vis spectrophotometric methods. The stability constant of the Gd^{3+} complex was determined by measuring the longitudinal relaxation times of the samples acquired in strongly acidic solutions. The measurements were performed with a Bruker Minispec MQ20 NMR analyzer (20 MHz, 25 °C) using the inversion recovery method (180° > τ > 90°) at 10 different τ values. Ten different samples were prepared containing $[Gd(octapa)]^-$ in 1 mM concentration, and the HCl concentration was varied in the concentration range of 0.05−0.5 M (pH = −log c_{H+}). The relaxometric competition method was used to verify the stability of the $[Gd(octapa)]^-$ complex. Samples containing 1 mM $[Gd(octapa)]^-$ and varying concentrations of the ttha^{6-} ligand (concentration range 1−20 mM, eight different samples) were prepared and equilibrated at pH = 8.1 (I = 0.15 M NaCl). The T_1 relaxation times of the samples were then recorded and fitted by using the molar relaxivities of the $[Gd(octapa)]^-$ and $[Gd(ttha)]^{3-}$ complexes determined independently (5.49 mM^{-1} s^{-1} and 2.43 mM^{-1} s^{-1} at 25 °C and 20 MHz, respectively). The protonation constants of the ttha^{6-} ligand as well as the protonation and stability constants of the complexes used in the fittings are included in the Supporting Information (Table S3).

In possession of the verified stability constant of the $[Gd(octapa)]^-$ complex the stabilities of $[La(octapa)]^-$, $[Lu(octapa)]^-$, and $[Zn(octapa)]^{2-}$ were calculated by using competition reactions occurring between the $[Gd(octapa)]^-$ complex and La^{3+}, Lu^{3+}, and Zn^{2+} ions. A total of seven samples containing 1 mM $[Gd(octapa)]^-$ and 0.5−20 mM (La^{3+}), 0.25−10 mM (Lu^{3+}), or 0.25−30 mM (Zn^{2+}) metal chlorides were prepared and equilibrated at constant pH 5.3 for La^{3+} and Lu^{3+} and 5.7 for Zn^{2+}. Longitudinal relaxation times of the samples were then measured, and the formation constants were determined by using the relaxivities of the Gd^{3+} aqua ion and $[Gd(octapa)]^-$ (13.27 mM^{-1} s^{-1} and 5.49 mM^{-1} s^{-1} at 25 °C and 20 MHz, respectively). The formation constant of the La^{3+} complex was also confirmed by UV−vis spectrophotometry measurements performed in highly acidic solutions of the complexes by following the changes in the absorption band of the picolinate moiety (287−306 nm, 1 cm Hellma quartz cells). The concentration of $[La(octapa)]^-$ in the samples (total 10 samples) was set to 0.5 mM, while acid concentration was varied in the range of 0.005−0.5 M. The molar absorption coefficients of the absorbing species (octapa^{4-} and $[La(octapa)]^-$) were determined independently from the spectra recorded at three different concentrations.

Because of the high conditional stability of $[Cu(octapa)]^{2-}$ the formation of the complex is almost 100% even in 1 M HCl solution. For this reason, the competition between the octapa^{4-} and cyclen ligands for Cu^{2+} was used to determine the stability constant of $[Cu(octapa)]^{2-}$. A total of eight samples were prepared containing 2 mM $[Cu(octapa)]^{2-}$ and varying the concentration of cyclen in the range of 1−20 mM (the pH of the samples were in the range of 10−11). The stability constant of the $[Cu(cyclen)]^{2+}$ complex and the molar absorptivity of the complexes were determined independently in the wavelength range of 500−720 nm (1 cm Hellma cells with the use of Varian Cary 1E, UV−visible spectrophotometer) by using standard methodology. The stability constants of the complexes were calculated with the PSEQUAD program.[38]

Kinetic Measurements. The rates of the metal exchange reactions of the $[Gd(octapa)]^-$ complex were studied by using UV−vis spectrophotometry following the formation of the $[Cu(octapa)]^{2-}$ complex. The metal exchange reactions of $[Gd(octapa)]^-$ were studied by a stopped-flow method (Applied Photophisics DX-17MV stopped-flow machine) because the decomplexation of $[Gd(octapa)]^-$ was found to be fast for the time scale of the conventional spectrophotometric methods. The exchange reactions were followed at 250 nm in the pH range of 3.6−5.0. To evaluate the rate constant characterizing the acid-catalyzed dissociation reactions, exchange reactions were also studied in the $[H^+]$ range of 0.01−0.1 M. The concentration of the complex was 0.05 mM, while the Cu^{2+} ion was applied at high excess (10 to 50 fold) to ensure pseudo-first-order conditions. The temperature was maintained at 25 °C, and the ionic strength of the solutions was kept constant by using 0.15 M NaCl. For keeping the pH constant, dimethylpiperazine (20 mM) buffer was used (log K_2^H = 4.90) in the pH range of 3.6−5.0. The pseudo-first-order rate constants (k_{obs}) were calculated by fitting the absorbance versus time data to eq 10.

$$A_t = (A_0 - A_e)e^{-k_{obs}t} + A_e \quad (10)$$

where A_t, A_0, and A_e are the absorbance at time t, at the start, and at equilibrium of the reactions, respectively. The fittings were performed with the computer program Micromath Scientist, version 2.0 (Salt Lake City, UT, USA), by using a standard least-squares procedure. Each point on the figures showing kinetic data was obtained by averaging 5−6 rate constants obtained under identical conditions.

Computational Details. All calculations presented in this work were performed employing the Gaussian 09 package (Revision B.01).[39] Full geometry optimizations of the $[Ln(octapa)(H_2O)]^-\cdot 2H_2O$ systems were performed both in the gas phase and in aqueous solution employing DFT within the hybrid meta generalized gradient approximation (hybrid meta-GGA) with the TPSSh exchange-correlation functional.[40] Geometry optimizations were performed by using the large-core quasirelativistic effective core potential of Dolg and co. and its associated [5s4p3d]-GTO valence basis set,[41] while the ligand atoms were described by using the standard 6-31G(d,p) basis set. Input geometries were taken from a previous computational study on the Gd analogue.[31] Full geometry optimizations of the $[M(octapa)]^{2-}$ complexes (M = Zn or Cu) were carried out in aqueous solution using the TPSSh functional and the standard Ahlrich's triple-ξ basis set with polarization functions (TZVP).[42] No symmetry constraints were imposed during the optimizations. In the case of the copper complex calculations were performed by using an unrestricted model. The stationary points found on the potential energy surfaces as a result of geometry optimizations were tested to represent energy minima rather than saddle points via frequency analysis. The default values for the integration grid (75 radial shells and 302 angular points) and the self-consistent field energy convergence criteria (1×10^{-8}) were used in all calculations. Basis set superposition errors (BSSEs), which represent an undesirable consequence of using finite basis sets that leads to an overestimation of the binding energy, were calculated using the standard counterpoise method[43] with calculations performed in the gas phase.[44]

The NMR shielding tensors of the $[Zn(octapa)]^{2-}$ system were calculated in aqueous solution at the TPSSh/TZVP level by using the GIAO method.[45] For ^{13}C NMR chemical shift calculation purposes, the NMR shielding tensors of tetramethylsilane (TMS) were calculated at the same level.

Throughout this work solvent effects were included by using the polarizable continuum model, in which the solute cavity is built as an envelope of spheres centered on atoms or atomic groups with appropriate radii. In particular, the integral equation formalism variant

DOI: 10.1021/ic502966m
Inorg. Chem. XXXX, XXX, XXX−XXX

as implemented in Gaussian 09 was used.[46] Hydration free energies were obtained using the radii and nonelectrostatic terms obtained by Truhlar et al. (SMD solvation model),[47] except for the Ln^{3+} ions, for which we used the radii parametrized in our previous work.[25]

■ ASSOCIATED CONTENT

Ⓢ Supporting Information

^{1}H, ^{13}C NMR, mass spectra, and absorption spectra of the Cu^{2+}:octapa^{4-}:cyclen:H^{+} and La^{3+}:octapa^{4-}:H^{+} systems, quadratic fit of the average bond distances of the metal coordination environments, protonation and stability constants of reference systems, compositions of the samples used in stability constant determination, calculated bond distances of the metal coordination environments, and optimized Cartesian coordinates obtained with DFT calculations. This material is available free of charge via the Internet at http://pubs.acs.org.

■ AUTHOR INFORMATION

Corresponding Authors

*E-mail: carlos.platas.iglesias@udc.es. (C.P.-I.)
*E-mail: gyula.tircso@science.unideb.hu. (G.T.)

Notes

The authors declare no competing financial interest.

■ ACKNOWLEDGMENTS

C.P.-I. and M.R.-F. are indebted to Centro de Supercomputación de Galicia (CESGA) for providing the computer facilities. F.K.K., C.P.-I., É.J.T., and G.T. gratefully acknowledge support from the COST Actions CM1006 "European F-Element Network (EuFen)" and TD1004 "Theragnostics Imaging and Therapy: An Action to Develop Novel Nanosized Systems for Imaging-Guided Drug Delivery". F.K., A.V., and G.T. thank the Hungarian Scientific Research Fund (OTKA K-84291 and K-109029). G.T. and É.J.T gratefully acknowledge support from the Hungarian-French bilateral Scientific and Technological Cooperation (Project No. TÉT_11-2-2012-0010 and PHC Balaton). This work was also supported by the János Bolyai Research Scholarship (G.T.) of the Hungarian Academy of Sciences. The research was supported by the European Union and cofinanced by the European Social Fund under the Project TÁMOP 4.2.2.A-11/1/KONV-2012-0043.

■ REFERENCES

(1) *The Chemistry of Contrast Agents in Medical Magnetic Resonance Imaging*, 2nd ed.; Merbach, A. E., Helm, L., Tóth, É., Eds.; Wiley: New York, 2013.

(2) For recent reviews see: (a) Terreno, E.; Delli Castelli, D.; Viale, A.; Aime, S. *Chem. Rev.* **2010**, *110*, 3019−3042. (b) Kubicek, V.; Toth, E. *Adv. Inorg. Chem.* **2009**, *61*, 63−129. (c) Aime, S.; Delli Castelli, D.; Geninatti Crich, S.; Gianolio, E.; Terreno, E. *Acc. Chem. Res.* **2009**, *42*, 822−831. (d) Datta, A.; Raymond, K. N. *Acc. Chem. Res.* **2009**, *42*, 938−947. (e) Dorazio, S. J.; Morrow, J. R. *Eur. J. Inorg. Chem.* **2012**, 2006−2014.

(3) (a) Kueny-Stotz, M.; Garofalo, A.; Felder-Flesch, D. *Eur. J. Inorg. Chem.* **2012**, *12*, 1987−2005. (b) Drahos, B.; Lukes, I.; Toth, E. *Eur. J. Inorg. Chem.* **2012**, *12*, 1975−1986.

(4) Caravan, P.; Ellison, J.; McMurry, T.; Lauffer, R. *Chem. Rev.* **1999**, *99*, 2293−2352.

(5) Cheng, S.; Abramova, L.; Saab, G.; Turabelidze, G.; Patel, P.; Arduino, M.; Hess, T.; Kallen, A.; Jhung, M. *JAMA* **2007**, *297*, 1542−1544.

(6) Sarka, L.; Burai, L.; Brücher, E. *Chem.—Eur. J.* **2000**, *6*, 719−724.

(7) Platas-Iglesias, C.; Mato-Iglesias, M.; Djanashvili, K.; Muller, R. N.; Vander Elst, L.; Peters, J. A.; de Blas, A.; Rodríguez-Blas, T. *Chem.—Eur. J.* **2004**, *10*, 3579−3590.

(8) Chatterton, N.; Gateau, C.; Mazzanti, M.; Pecaut, J.; Borel, A.; Helm, L.; Merbach, A. E. *Dalton Trans.* **2005**, 1129−1135.

(9) Price, E. W.; Cawthray, J. F.; Bailey, G. A.; Ferreira, C. L.; Boros, E.; Adam, M. J.; Orvig, C. *J. Am. Chem. Soc.* **2012**, *134*, 8670−8683.

(10) Bailey, G. A.; Price, E. W.; Zeglis, B. M.; Ferreira, C. L.; Boros, E.; Lacasse, M. J.; Patrick, B. O.; Lewis, J. S.; Adam, M. J.; Orvig, C. *Inorg. Chem.* **2012**, *51*, 12575−12589.

(11) Ferreirós-Martínez, R.; Esteban-Gómez, D.; Platas-Iglesias, C.; de Blas, A.; Rodríguez-Blas, T. *Dalton Trans.* **2008**, 5754−5765.

(12) Boros, E.; Ferreira, C. L.; Cawthray, J. F.; Price, E. W.; Patrick, B. O.; Wester, D. W.; Adam, M. J.; Orvig, C. *J. Am. Chem. Soc.* **2010**, *132*, 15726−15733.

(13) Boros, E.; Cawthray, J. F.; Ferreira, C. L.; Patrick, B. O.; Adam, M. J.; Orvig, C. *Inorg. Chem.* **2012**, *51*, 6279−6284.

(14) (a) Price, E. W.; Zeglis, B. M.; Cawthray, J. F.; Lewis, J. S.; Adam, M. J.; Orvig, C. *Inorg. Chem.* **2014**, *53*, 10412−10431. (b) Price, E. W.; Zeglis, B. M.; Cawthray, J. F.; Ramogida, C. F.; Ramos, N.; Lewis, J. S.; Adam, M. J.; Orvig, C. *J. Am. Chem. Soc.* **2013**, *135*, 12707−12721.

(15) Price, E. W.; Cawthray, J. F.; Adam, M. J.; Orvig, C. *Dalton Trans.* **2014**, *43*, 7176−7190.

(16) Baranyai, Z.; Palinkas, Z.; Uggeri, F.; Brücher, E. *Eur. J. Inorg. Chem.* **2010**, 1948−1956.

(17) (a) Roca-Sabio, A.; Mato-Iglesias, M.; Esteban-Gomez, D.; Toth, E.; de Blas, A.; Platas-Iglesias, C.; Rodríguez-Blas, T. *J. Am. Chem. Soc.* **2009**, *131*, 3331−3341. (b) Palinkas, Z.; Roca-Sabio, A.; Mato-Iglesias, M.; Esteban-Gomez, D.; Platas-Iglesias, C.; de Blas, A.; Rodrıguez-Blas, T.; Toth, E. *Inorg. Chem.* **2009**, *48*, 8878−8889. (c) Roca-Sabio, A.; Bonnet, C. S.; Mato-Iglesias, M.; Esteban-Gómez, D.; Tóth, E.; de Blas, A.; Rodríguez-Blas, T.; Platas-Iglesias, C. *Inorg. Chem.* **2012**, *51*, 10893−10903. (d) Rodríguez-Rodríguez, A.; Garda, Z.; Ruscsák, E.; Esteban-Gómez, D.; de Blas, A.; Rodríguez-Blas, T.; Lima, L. M. P.; Beyler, M.; Tripier, R.; Tircsó, G.; Platas-Iglesias, C. *Dalton Trans.* **2015**, DOI: 10.1039/c4dt02985b.

(18) Szakács, Z.; Béni, S.; Noszál, B. *Talanta* **2008**, *74*, 666−674.

(19) The protonation constants of picolinic acid was determined in this work using potentiometric titrations in 0.15 M NaCl. Only one protonation constant could be determined log K_1^H = 5.26(2), as the second protonation constant is characterized by a log K_1^H < 1.

(20) Hancock, R. D.; Shaikjee, M. S.; Dobson, S. M.; Boeyens, J. C. A. *Inorg. Chim. Acta* **1988**, *154*, 229−238.

(21) Gritmon, T. F.; Goedken, M. P.; Choppin, G. R. *J. Inorg. Nucl. Chem.* **1977**, *39*, 2021−2023.

(22) Duffield, J. R.; May, P. M.; Williams, D. R. *J. Inorg. Biochem.* **1984**, *20*, 199−214.

(23) Korsse, J.; Pronk, L. A.; Van Embden, C.; Leurs, G.; Louwrier, P. W. F. *Talanta* **1983**, *30*, 1−7.

(24) Moeller, T.; Thompson, L. C. *J. Inorg. Nucl. Chem.* **1962**, *24*, 499−510.

(25) Regueiro-Figueroa, M.; Esteban-Gómez, D.; de Blas, A.; Rodríguez-Blas, T.; Platas-Iglesias, C. *Chem.—Eur. J.* **2014**, *20*, 3974−3981.

(26) Brücher, E.; Tircsó, G.; Baranyai, Z.; Kovács, Z.; Sherry, A. D. Stability and Toxicity of Contrast Agents. In *The Chemistry of Contrast Agents in Medical Magnetic Resonance Imaging*, 2nd ed.; Merbach, A. E., Helm, L., Tóth, É., Eds.; John Wiley & Sons, Ltd: Chichester, U.K., 2013; Ch 4, pp 157−208.

(27) Baranyai, Z.; Pálinkás, Z.; Uggeri, F.; Maiocchi, A.; Aime, S.; Brücher, E. *Chem.—Eur. J.* **2012**, *18*, 16426−16435.

(28) Brücher, E.; Szarvas, P. *Inorg. Chim. Acta* **1970**, *4*, 632−636.

(29) Brücher, E., Ph.D. Thesis, Kossuth Lajos University: Debrecen, 1981.

(30) (a) Jarvis, N. N.; Wagener, J. M.; Jackson, G. E. *J. Chem. Soc., Dalton Trans.* **1995**, 1411−1415. (b) Rösch, F.; Forssell-Aronsson, E. In *Metal Ions in Biological Systems*, Sigel, A., Sigel, H., Eds.; Marcel Decker Inc.: Basel, New York, 2004; Vol. *4*, pp 77−108.

(31) Esteban-Gomez, D.; de Blas, A.; Rodríguez-Blas, T.; Helm, L.; Platas-Iglesias, C. *ChemPhysChem* **2012**, *13*, 3640−3650.

DOI: 10.1021/ic502966m
Inorg. Chem. XXXX, XXX, XXX−XXX

(32) Seitz, M.; Oliver, A. G.; Raymond, K. N. *J. Am. Chem. Soc.* **2007**, *129*, 11153−11160.
(33) Platas, C.; Avecilla, F.; de Blas, A.; Rodriguez-Blas, T.; Bastida, R.; Macias, A.; Rodriguez, A.; Adams, H. *J. Chem. Soc., Dalton Trans.* **2001**, 1699−1705.
(34) (a) Guillaumont, R.; David, F. *Radiochem. Radioanal. Lett.* **1974**, *17*, 25−39. (b) Cosentino, U.; Villa, A.; Pitea, D.; Moro, G.; Barone, V. *J. Phys. Chem. B* **2000**, *104*, 8001−8007.
(35) Lever, A. B. P. *Inorganic Electronic Spectroscopy,* 2nd ed.; Elsevier: Amsterdam, 1984; pp 554−572.
(36) Beynon, R. J.; Easterby, J. S. In *Buffer Solutions: The Basics;* Oxford University Press: New York, 1996.
(37) Irving, H. M.; Miles, M. G.; Pettit, L. *Anal. Chim. Acta* **1967**, *38*, 475−488.
(38) Zékány, L.; Nagypál, I. In *Computational Method for Determination of Formation Constants,* Legett, D. J., Ed.; Plenum: New York, 1985; p 291.
(39) Frisch, M. J.; Trucks, G. W.; Schlegel, H. B.; Scuseria, G. E.; Robb, M. A.; Cheeseman, J. R.; Scalmani, G.; Barone, V.; Mennucci, B.; Petersson, G. A.; Nakatsuji, H.; Caricato, M.; Li, X.; Hratchian, H. P.; Izmaylov, A. F.; Bloino, J.; Zheng, G.; Sonnenberg, J. L.; Hada, M.; Ehara, M.; Toyota, K.; Fukuda, R.; Hasegawa, J.; Ishida, M.; Nakajima, T.; Honda, Y.; Kitao, O.; Nakai, H.; Vreven, T.; Montgomery, J. A., Jr.; Peralta, J. E.; Ogliaro, F.; Bearpark, M.; Heyd, J. J.; Brothers, E.; Kudin, K. N.; Staroverov, V. N.; Kobayashi, R.; Normand, J.; Raghavachari, K.; Rendell, A.; Burant, J. C.; Iyengar, S. S.; Tomasi, J.; Cossi, M.; Rega, N.; Millam, N. J.; Klene, M.; Knox, J. E.; Cross, J. B.; Bakken, V.; Adamo, C.; Jaramillo, J.; Gomperts, R.; Stratmann, R. E.; Yazyev, O.; Austin, A. J.; Cammi, R.; Pomelli, C.; Ochterski, J. W.; Martin, R. L.; Morokuma, K.; Zakrzewski, V. G.; Voth, G. A.; Salvador, P.; Dannenberg, J. J.; Dapprich, S.; Daniels, A. D.; Farkas, Ö.; Foresman, J. B.; Ortiz, J. V.; Cioslowski, J.; Fox, D. J. *Gaussian 09,* Revision A.01; Gaussian, Inc.: Wallingford, CT, 2009.
(40) Tao, J. M.; Perdew, J. P.; Staroverov, V. N.; Scuseria, G. E. *Phys. Rev. Lett.* **2003**, *91*, 146401.
(41) Dolg, M.; Stoll, H.; Savin, A.; Preuss, H. *Theor. Chim. Acta* **1989**, *75*, 173−194.
(42) Schaefer, A.; Huber, C.; Ahlrichs, R. *J. Chem. Phys.* **1994**, *100*, 5829−5835.
(43) Bernardi, F.; Boys, S. F. *Mol. Phys.* **1970**, *19*, 553−566.
(44) Zawada, A.; Gora, R. W.; Mikolajczyk, M. M.; Bartkowiak, W. *J. Phys. Chem. A* **2012**, *116*, 4409−4416.
(45) Ditchfield, R. *Mol. Phys.* **1974**, *27*, 789−807.
(46) Tomasi, J.; Mennucci, B.; Cammi, R. *Chem. Rev.* **2005**, *105*, 2999−3093.
(47) Marenich, A. V.; Cramer, C. J.; Truhlar, D. G. *J. Phys. Chem. B* **2009**, *113*, 6378−6396.

DOI: 10.1021/ic502966m
Inorg. Chem. XXXX, XXX, XXX−XXX